79-4026

Total Pressure Recovery of Flared Fan Nozzles Used as Inlets

T.G. Keith Jr.* and T.N. Obee†
University of Toledo, Toledo, Ohio
and
D.A. Dietrich‡
Texas A&M University, College Station, Texas

A simple expression has been developed which accurately represents the total pressure recovery of a flared exhaust nozzle when it is used as an inlet. Physically such a situation can arise during the reverse-thrust operation of a variable pitch fan jet. The formula is written in terms of the freestream and duct Mach numbers and contains two empirical coefficients. One coefficient is associated with internal flow losses in the nozzle and can be found from a static engine test. The other coefficient is associated with flow losses in the external field of the nozzle and can be approximated from existing cone drag data. The developed expression produces an excellent fit of measured total pressure recoveries; differences between calculated and experimental values were generally less than 0.5%.

Nomenclature

A_o/A_d = contraction ratio: area ratio of the exlet opening to the fan duct
C/C^* = ratio of experimental to theoretical drag coefficient for a cone (Ref. 6)
C_p = wake pressure coefficient
K_e = external loss coefficient
K_i = internal loss coefficient
M_d = fan duct Mach number
M_∞ = freestream Mach number
P = static pressure
P_t = total pressure
q = dynamic pressure
γ = specific heat ratio
θ = flare angle

Subscripts

d = exlet fan duct
o = exlet opening
w = exlet wake
∞ = freestream

Superscripts

$(\hat{})$ = nondimensional
$(\bar{})$ = arithmetic average

I. Introduction

A NOVEL thrust-reverser system is being examined for use on the quiet clean short-haul experimental engine (QCSEE). Figure 1 is a diagram of this high-bypass variable pitch fan jet operating in reverse thrust. To accomplish thrust reversal, the fan blade pitch is reversed and air is pulled into the nacelle through the fan exhaust nozzle which has been purposely flared. Since, during this mode of engine operation, the exhaust nozzle will function as an inlet, and for convenience when it is so employed, we will refer to it as an exlet.

Since the direction of the external freestream flow is opposite that of the internal flow, the operating characteristics of an exlet may be expected to differ from those of an inlet facing upstream. This, in turn, suggests the need for a method of performance prediction that is appropriate for the exlet.

In any discussion of exlet performance, total pressure recovery (percent of the freestream total pressure available after the flow has passed through the exlet) is surely to be of major concern. This parameter is directly related to the level of reverse thrust developed by a variable pitch fan in a nacelle. Furthermore, the exlet total pressure recovery affects the power available from the engine core. Although exlet total pressure recovery is an important performance parameter, it presently exists only as uncorrelated wind tunnel data, which makes any subsequent use difficult. The purpose of this paper is to remedy this situation by developing expressions which can be used to predict exlet total pressure recovery over a wide range of operating conditions.

In the following, a mass-momentum balance approach will be first considered. It was found that this method could be used to estimate the total pressure recovery of nonflared sharp-lip exlets. However, the same method could not be as conveniently used to predict pressure recoveries of more realistic conically flared exlets because the analysis resulted in expressions which contained integrals of the static pressure over the exlet boundaries. Inability to evaluate these pressure integrals caused attention to be directed toward an alternate procedure and a semiempirical expression for exlet total pressure recovery was developed. The expression contains two loss coefficients which were evaluated by utilizing the existing wind tunnel data of Refs. 1 and 2. Moreover, the expression was an outgrowth of earlier analytical studies of Refs. 3-5, and is based on simple representations of flow losses.

II. Analysis

A. Mass-Momentum Balance Approach for Nonflared Sharp-Lip Exlets

Figure 2 is a sketch of the flowfield in the vicinity of a nonflared exlet. It is assumed that the duct is very long so that a uniform velocity exists both at the entry and exit regions of the flowfield. The interaction between the freestream flow and the flow being drawn into the exlet results in a stagnation point downstream of the exlet. Water table model studies carried out in Ref. 5 provide a two-dimensional verification of the occurrence of this stagnation point. Streamlines which pass through the point define a stagnation surface that divides the flowfield into two parts. Inside the stagnation surface, fluid is drawn into the exlet. This flow experiences a drop in total pressure because of losses associated with the flow

Received Feb. 6, 1978; revision received June 30, 1978. Copyright © American Institute of Aeronautics and Astronautics, Inc., 1978. All rights reserved.

Index categories: Nozzle and Channel Flow; Subsonic Flow.

*Associate Professor. Member AIAA.
†Graduate Assistant.
‡Assistant Professor. Member AIAA.

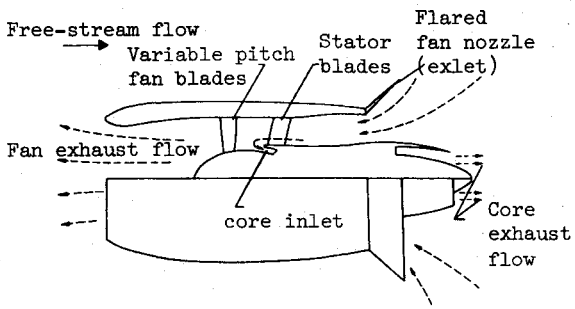

Fig. 1 Elements of a variable-pitch fan engine during reverse thrust operation.

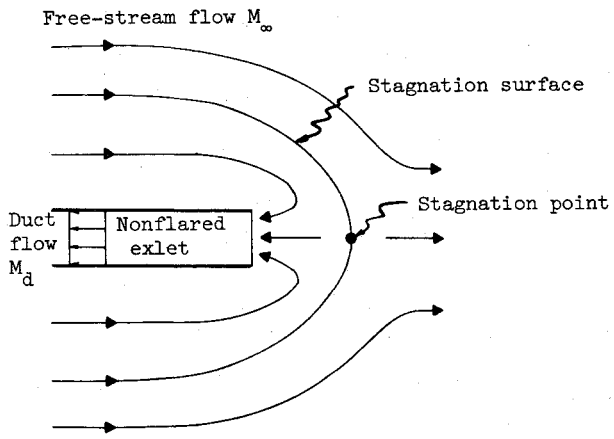

Fig. 2 Flowfield in the vicinity of a nonflared sharp-lip exlet.

separation that inevitably occurs at the exlet lip when the flow is turned into the flared opening. Outside the stagnation surface, fluid passes by without any reduction of the total pressure and therefore the outer field is taken to be irrotational and isotropic.

In Ref. 4 the dividing stagnation surface was used as a control-volume boundary and a mass-momentum balance was performed on the internal flow. The resulting expression involved two pressure integrals: one associated with the suction force on the exlet lip and the other with the pressure drag on the stagnation stream surface. However, for a nonflared exlet having a lip of theoretically zero thickness, there is no area to support the suction force and the corresponding pressure integral vanishes for such a hypothetical device. Moreover, because the external flow acting on the stagnation surface is isentropic, the drag on this surface has been shown in Ref. 3 to be zero.

Incorporation of these ideas into the mass-momentum balance leads to an expression for the total pressure recovery, $P_{td}/P_{t\infty}$. The expression can be written solely in terms of the fan duct Mach number M_d, the freestream Mach number M_∞, and the ratio of specific heats γ. It is derived in Ref. 4 and presented here as Eq. (1):

$$\frac{P_{td}}{P_{t\infty}} = \left(\frac{1+M_d^2(\gamma-1)/2}{1+M_\infty^2(\gamma-1)/2}\right)^{\gamma/(\gamma-1)} \left[1+\gamma M_d^2 + \gamma M_\infty M_d \left(\frac{1+M_d^2(\gamma-1)/2}{1+M_\infty^2(\gamma-1)/2}\right)^{1/2}\right]^{-1} \quad (1)$$

To extend this method to the more realistic case of a conically flared exlet requires that the distribution of static pressure be known along the flared exlet boundary. However, that information was not available and could not be simply estimated, hence an alternate approach was considered.

B. Loss Coefficient Approach to Flared Exlets

The approach used in the analysis which follows is to introduce empirical constants to represent the performance of conically flared exlets. These constants correspond to the loss coefficients for two basic types of flow losses: one is related to the internal flow which can be characterized by the fan duct Mach number M_d, and the other is related to the external flow characterized by the freestream Mach number M_∞. Figure 3 depicts the geometry and nomenclature of the two flow types.

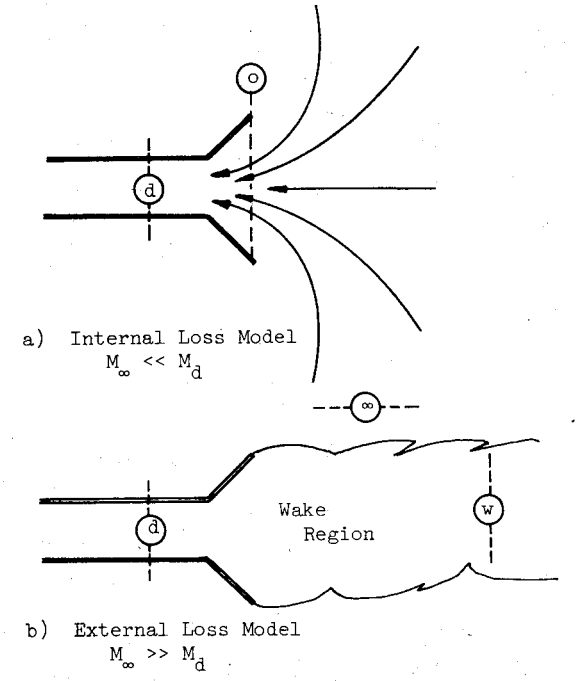

Fig. 3 Geometry and nomenclature of the internal and external loss models.

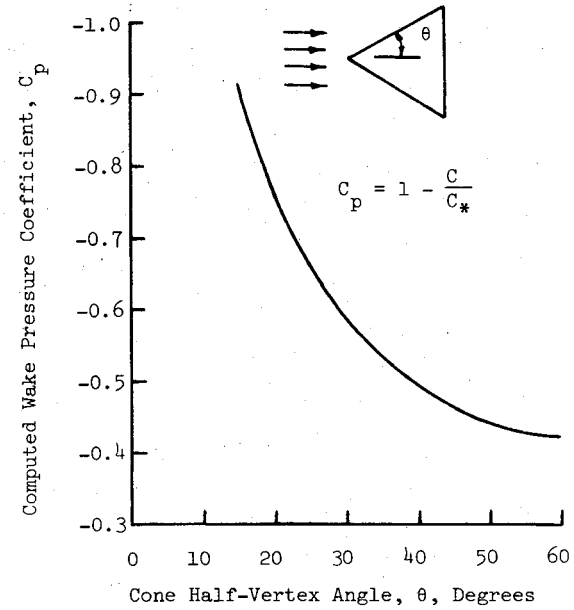

Fig. 4 Wake pressure coefficient for an upstream facing cone vs cone half-vertex angle.

Internal Losses

In fluid mechanics, it is common practice to account for internal flow losses through the use of a loss coefficient. This parameter must generally be established experimentally and has been found to be a strong function of the flow geometry. Values corresponding to typical flow situations can be found in most elementary fluid mechanics texts, e.g., see Ref. 7.

An internal loss coefficient may be defined as follows:

$$K_i \equiv (P_{to} - P_{td})/q_d \quad (2)$$

where $(P_{to}-P_{td})$ refers to the total pressure loss associated with the contracted flow that enters the exlet and q_d refers to the dynamic pressure of the duct flow. The latter may also be written as $\gamma M_d^2 P_d/2$. Multiplying Eq. (2) by q_d/P_{td} and solving for the total pressure ratio P_{td}/P_{to} leads to

$$\frac{P_{td}}{P_{to}} = \hat{P}_{t\,\text{internal}} = \frac{1}{1+K_i(\gamma M_d^2/2)(P/P_t)_d}$$

But the static to total pressure ratio is

$$\frac{P}{P_t} = \left(1+\frac{\gamma-1}{2}M^2\right)^{-\gamma/(\gamma-1)} \tag{3}$$

Thus

$$\hat{P}_{t\,\text{internal}} = \frac{1}{1+K_i(\gamma M_d^2/2)(1+M_d^2(\gamma-1)/2)^{-\gamma/(\gamma-1)}} \tag{4}$$

When an exlet (flared or nonflared) is operating in a quiescent or nearly quiescent field, $M_\infty \simeq 0$, and it may be expected that Eq. (4) can be used to estimate exlet total pressure recovery. This follows from the fact that in a nearly static field the total pressure in the vicinity of the exlet opening is approximately equal to the freestream total pressure.

Although Eq. (4) contains only M_d, γ, and K_i, it is anticipated that K_i will vary both with exlet geometry and local flow conditions. To obtain an impression concerning the latter, the total pressure recovery for a nonflared exlet in a quiescent field, i.e., Eq. (1) with $M_\infty = 0$, is equated to Eq. (4) and K_i is found to be

$$K_i = \frac{2}{\gamma M_d^2}\left[1+\gamma M_d^2 - \left(1+\frac{\gamma-1}{2}M_d^2\right)^{\gamma/(\gamma-1)}\right]$$

In the present study, $0<M_d<0.5$; for this range of duct Mach numbers, $1.0>K_i>0.937$. Thus we may conclude from this evaluation of a nonflared exlet that the internal loss coefficient is not a strong function of M_d and, consequently, a single value of K_i can be used to represent the variation due to M_d. Of course, effects of geometry remain to be assessed.

External Losses

When the freestream flow is of sufficient strength to override the suction effects of the duct flow, a wake region with lower total pressure $(P_{tw}<P_{t\infty})$ forms behind the flared exlet opening. The limiting case of this flow type occurs when the fan is not running, i.e., when $M_d=0$. In fact, this flow condition represents the opposite extreme to the static freestream case.

To account for losses that occur when a region of separated flow stands behind the exlet, an external loss coefficient is defined as

$$K_e \equiv (P_w - P_\infty)/q_\infty \tag{5}$$

Physically, K_e represents the losses that occur between the external freestream and the intake flow stream prior to entering the flared portion of the exlet. By multiplying both sides of Eq. (5) by $(q_\infty/P_\infty)(P_{tw}/P_{t\infty})$ and rearranging the result, we find that

$$\frac{P_{tw}}{P_{t\infty}} = \frac{(P/P_t)_\infty}{(P/P_t)_w}\left(1+K_e\frac{\gamma M_\infty^2}{2}\right)$$

In general, the Mach number associated with the flow in the wake region or that in the vicinity of the exlet, i.e., M_w, will not be large; hence, to a reasonable degree of accuracy, it may be assumed that $P_{tw} \simeq P_w$. This, along with the employment of Eq. (5), permits the previous equation to be expressed as

$$\frac{P_{tw}}{P_{t\infty}} \equiv \hat{P}_{t\,\text{external}} = \left(1+K_e\frac{\gamma M_\infty^2}{2}\right)\left(1+\frac{\gamma-1}{2}M_\infty^2\right)^{-\gamma/(\gamma-)} \tag{6}$$

Like the internal loss coefficient, K_e may be expected to vary with the exlet geometry and flow conditions. However, because of the very nature of the parameter, flow conditions should have a more pronounced effect on K_e than on K_i. Certainly, the most practical means of evaluating K_e is by experiment. A conically flared exlet has a shape resembling an upstream facing cone. Moreover, when the fan is not running, K_e equals the wake pressure coefficient C_p. In fact, K_e was defined in such a way that this would be the case. Therefore, the published cone drag data of Ref. 6 can be used to estimate K_e. Figure 4 is a plot of these computed coefficients and for cases where M_d is small, K_e may be read from that figure.

It should be noted that Eq. (6) does not represent exlet total pressure recovery except in cases where $P_{tw} \simeq P_{to} \simeq P_{td}$ which can occur in situations of very small duct Mach numbers. In cases of larger M_d, internal losses may be expected to become important, i.e., $P_{td}<P_{to}$, and must therefore be taken into account. Because of this, a combined loss model was devised.

Combined Losses

The exlet total pressure recovery including both internal and external losses is taken to be

$$\frac{P_{td}}{P_{t\infty}} = \frac{P_{td}}{P_{to}} \times \frac{P_{to}}{P_{tw}} \times \frac{P_{tw}}{P_{t\infty}} = \hat{P}_{t\,\text{internal}}\left(\frac{P_{to}}{P_{tw}}\right)\hat{P}_{t\,\text{internal}}$$

Assuming $P_{to} \simeq P_{tw}$ for all flows and inserting Eqs. (4) and (6) yields

$$\frac{P_{td}}{P_{t\infty}} = \frac{\left(1+K_e\frac{\gamma M_\infty^2}{2}\right)\left(1+\frac{\gamma-1}{2}M_\infty^2\right)^{-\gamma/(\gamma-1)}}{1+K_i\frac{\gamma M_d^2}{2}\left(1+\frac{\gamma-1}{2}M_d^2\right)^{-\gamma/(\gamma-1)}} \tag{7}$$

Notice that this expression contains both the $M_\infty=0$ and $M_d=0$ limiting flow cases. For the static freestream situation, $M_\infty=0$, $P_{\text{external}}\to 1$, and Eq. (7) yields Eq. (4); whereas for the case when the fan is shut off, $M_d=0$, $\hat{P}_{\text{internal}}\to 1$, and Eq. (6) is obtained with $K_e=C_p$.

Table 1 Exlet configuration details and computed internal loss coefficients

Curve symbol	Flare angle θ, deg	Contraction ratio A_o/A_d	Calculated internal loss coefficient $\bar{K}_i$	Ref.
○	45	2.11	0.093	1
□	30	1.74	0.063	1
◇	60	2.11	0.215	1
△	30	2.11	0.035	1
▷	45	1.51	0.084	1
▷	45	2.74	0.150	1
▷	60	2.41	0.252	1
◇◑●	0	1.00	1.30	1
○	30	1.74	0.084	2
□	36	1.96	0.087	2
◇	20	1.40	0.112	2
△	25	1.74	0.087	2
▷	36	1.74	0.087	2
▷	25	1.62	0.090	2
▷	30	1.62	0.088	2
◇	30	1.96	0.082	2
△	20	1.58	0.096	2

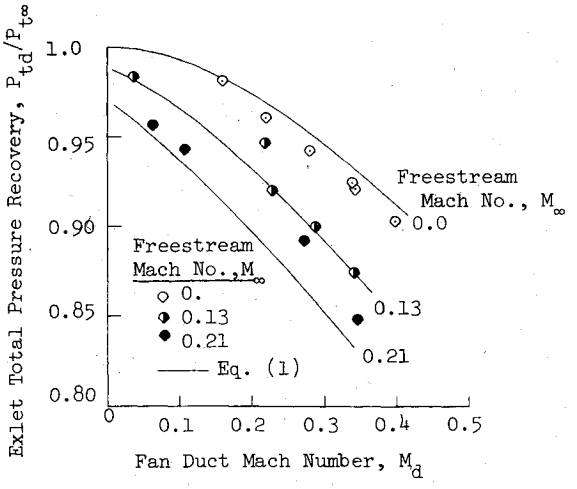

Fig. 5 Comparison of calculated total pressure recovery of a nonflared exlet with experimental data for various freestream Mach numbers.

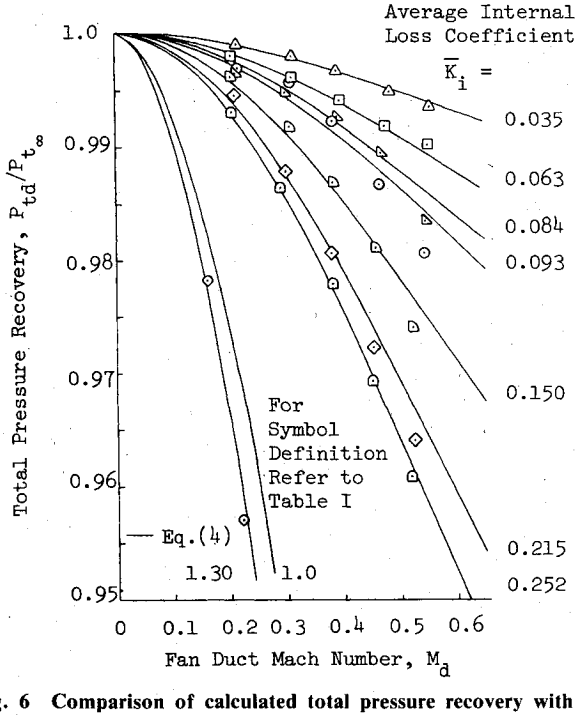

Fig. 6 Comparison of calculated total pressure recovery with experimental data in a quiescent freestream.

III. Results and Discussion

In this section, the existing experimental exlet total pressure recovery data of Refs. 1 and 2 were used to compute magnitudes of the undetermined coefficients K_i and K_e, and to test the validity of the proposed formula. Table 1 summarizes the pertinent information concerning the varieties of exlets used in these evaluations.

A. Mass-Momentum Balance Approach

As has been mentioned, in the case of flow past a nonflared, sharp-lip exlet, a mass-momentum balance can be used to obtain an expression for exlet total pressure recovery; that expression appears as Eq. (1). In Fig. 5, the theoretical predictions of Eq. (1) are compared to the nonflared exlet wind tunnel data of Ref. 1 for three freestream Mach numbers: 0, 0.13, and 0.21. Agreement between theoretical and experimental values is 4% or less. Measured recoveries lower than predicted in the static freestream case are attributed to the fact that the exlet used in the experiment had additional internal losses not accounted for in the idealized exlet mass-momentum analysis. On the other hand, measured recoveries greater than predicted at the highest M_∞ value are thought to be associated with unaccounted for separated flow losses involved with the formation of a wake region behind the exlet.

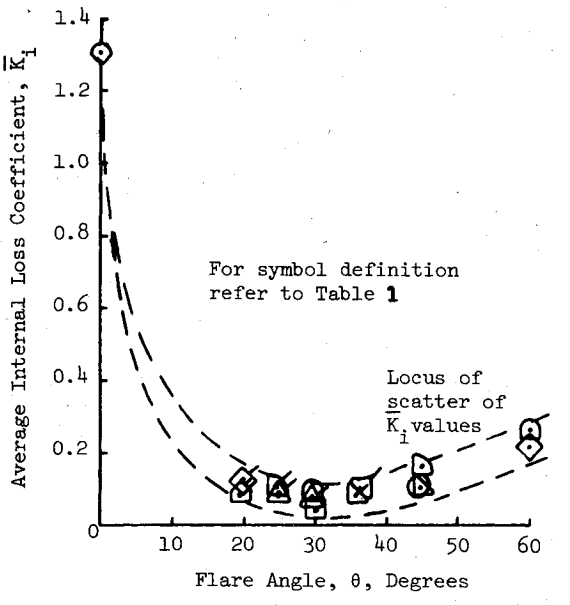

Fig. 7 Average internal loss coefficient vs exlet flare angle.

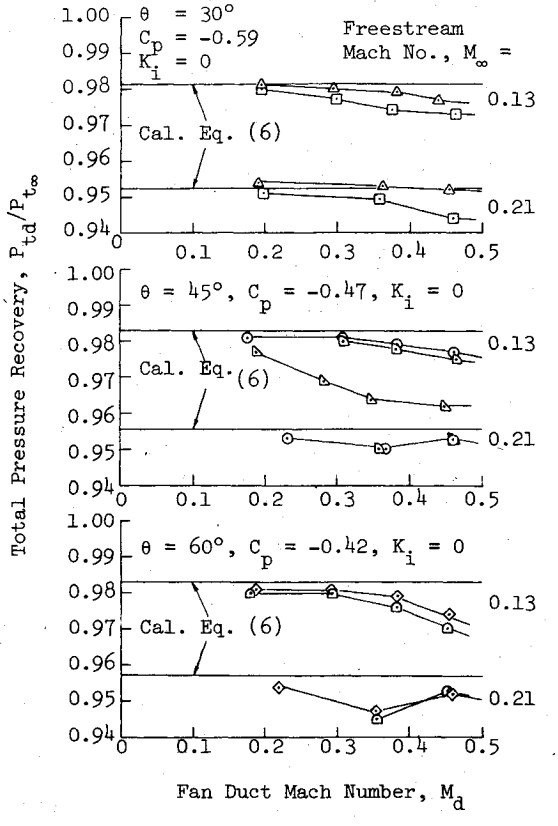

Fig. 8 Comparison of calculated total pressure recovery with experimental data for two freestream Mach numbers and three exlet flare angles.

B. Loss-Coefficient Approach

Internal Losses

Because Eq. (4) can be interpreted as the exlet total pressure recovery obtainable in a quiescent freestrean, it can be used to evaluate the internal loss coefficient, K_i. Experimental values of M_d and $P_{td}/P_{t\infty}$ were inserted into Eq. (4) and a set of K_i for each particular exlet was obtained. A simple arithmetic

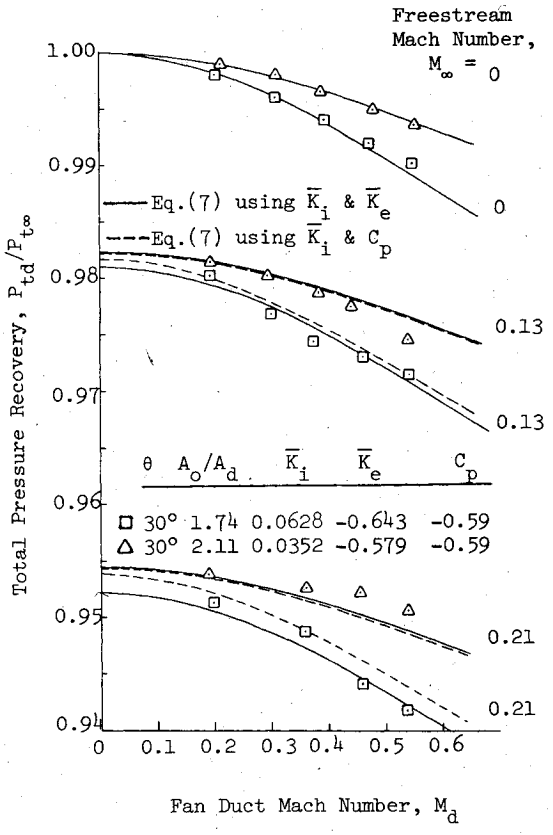

Fig. 9 Comparison of calculated total pressure recovery assuming no internal losses with experimental data for two 30-deg flared exlets at various freestream Mach numbers.

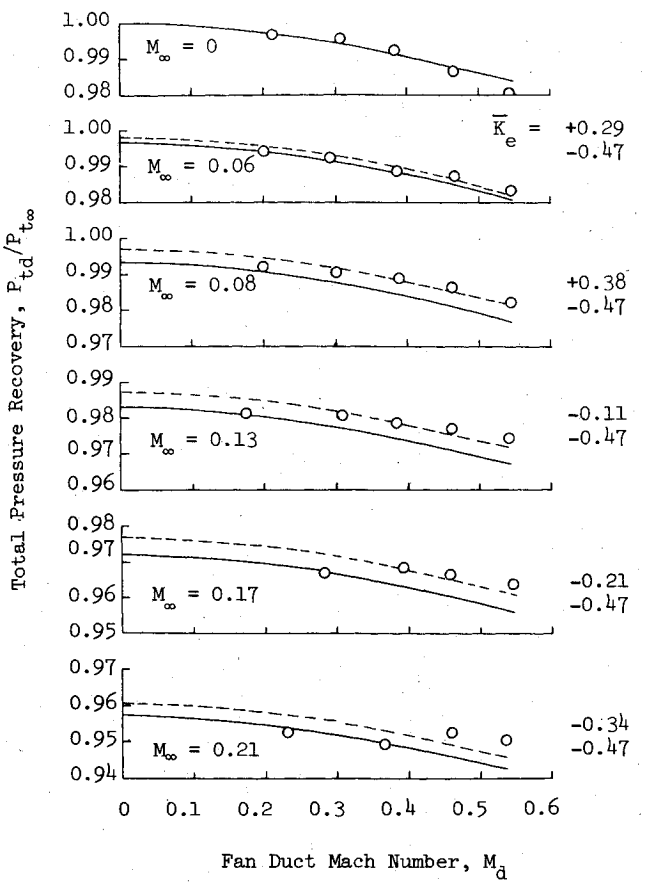

Fig. 10 Comparison of calculated total pressure recovery with experimental data for a 45-deg flared exlet at various freestream Mach numbers.

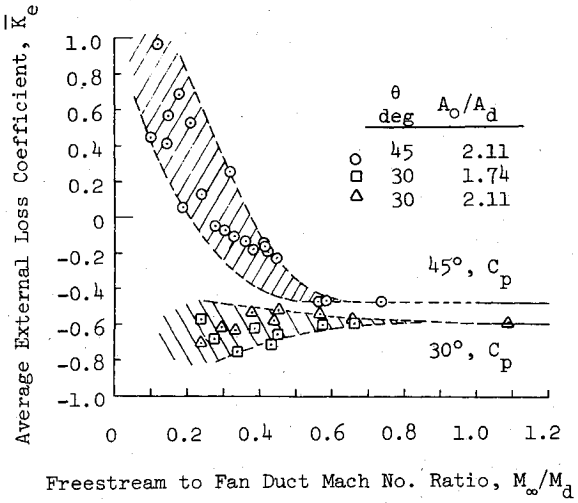

Fig. 11 Variation of the average external loss coefficient with the freestream to duct Mach number ratio.

average of these calculated values produced an average internal loss coefficient $\bar{K}_i$ for each exlet and is displayed in Table 1.

Figure 6 is a plot of the total pressure recovery against fan duct Mach number for a variety of exlets that were operated at static conditions. It can be seen that the general shape of the experimental data was obtained, and that the predicted values are within 0.5% of the corresponding experimental points. It may be concluded that Eq. (4) accurately describes total pressure recovery for given values of M_d and $\bar{K}_i$ at static freestream conditions.

Figure 7 displays the variation of computed $\bar{K}_i$ with flare angle for a variety of exlets. The dotted curves on the figure give an indication of the scatter of the values. This figure shows that $\bar{K}_i$ tends toward a minimum value, and hence a maximum in performance, around a flare angle of 30 deg. The variation due to contraction ratio, A_0/A_d, for the 30-deg flared exlets shown in Table 1 has little effect on $\bar{K}_i$ and hence on pressure recovery.

External Losses

Figure 8 is a series of plots of experimental exlet total pressure recovery against M_d for selected values of M_∞ and exlet flare angle. Constant total pressure recovery limits are drawn on the figure using Eq. (6) and a value of the external loss coefficient K_e set equal to the wake pressure coefficient C_p of Fig. 4. The predicted pressure recovery is seen to approximate the experimental data of Ref. 1 at low values of M_d. The measured values are lower than predicted for high values of M_d. There are two reasons for the disparity. First, high fan duct Mach numbers cause a collapse of the wake region behind the exlet, and therefore $K_e \neq C_p$. Second, high values of M_d result in exlet intake flow losses which have not been taken into account but which can be accounted for by use of a combined loss approach.

Combined Losses

Internal and external flow losses were combined in Eq. (7) to give a formula for exlet total pressure recovery applicable for a wide set of flow conditions. The equation contains both the internal and external loss coefficients. However, it was assumed that forward velocity has a second-order effect on $\bar{K}_i$ and therefore the internal loss coefficient evaluated from the static freestream experimental data was used directly. In effect this assumption uncouples the loss coefficients and permits each to be determined separately.

Inserting the static value of $\bar{K}_i$ into Eq. (7) along with experimental data points permits a set of K_e values to be determined for each exlet. A simple arithmetic average gave: $\bar{K}_e = -0.643$ for the low-area-ratio 30-deg flared exlet and

$\bar{K}_e = -0.579$ for the high-aspect-ratio 30-deg flared exlet. The solid curves in Fig. 9 are computed total pressure recoveries using these $\bar{K}_e$ and $\bar{K}_i$ values in Eq. (7). It can be seen that the semiempirical curves follow the experimental data very well; differences between them are less than 0.2%. For comparative purposes, a set of dashed curves were drawn in Fig. 9. These curves were computed from Eq. (7) using the appropriate $\bar{K}_i$ and K_e set equal to C_p as determined from cone wake pressure data. Obviously the predicted recoveries do not differ significantly from those based on average values of $\bar{K}_e$.

Figure 10 was drawn in order to confirm the above findings for an exlet with a larger flare angle. This figure is a series of plots of total pressure recovery for a 45-deg flared exlet as a function of fan duct Mach number for six freestream Mach numbers. An average internal loss coefficient of 0.093, determined from static freestream wind tunnel data, was used in all calculations. As with the 30-deg flared exlet, appropriate values of $\bar{K}_e$ were determined from the experimental data assuming that K_i and K_e could be uncoupled. The values obtained allowed the solid curves in Fig. 10 to be drawn. Also shown in the plot are the curves corresponding to $K_e = C_p = -0.47$ which was read from Fig. 4. Again, good representation of the experimental data was obtained; differences are less than 0.5%.

It comes as somewhat of a surprise that although $\bar{K}_e$ differs considerably from C_p for the 45-deg flared exlet, the corresponding pair of curves in Fig. 10 are rather close together. The reason for this is that the largest difference between C_p and $\bar{K}_e$ occurs at the smallest freestream Mach numbers. And since $\bar{K}_e$ appears only as the coefficient of M_∞^2, in Eq. (7), large differences in the values do not greatly affect the total pressure recovery for small values of M_∞. Alternately, for high values of M_∞, $\bar{K}_e$ values tend toward C_p provided the fan duct Mach number is not too large. Thus it appears that Eq. (7) has a built-in feature that does not allow $\bar{K}_e$ to overcorrect freestream effects. Figure 11 was drawn to illustrate this $\bar{K}_e$ variation. It is a plot of the average external loss coefficient for both the 30- and 45-deg flared exlets of Fig. 9 and 10 against the freestream to fan duct Mach number ratio, M_∞ / M_d.

As a final point, it should be mentioned that other exlet experimental data of Refs. 1 and 2 were fit in the same manner as that shown here. In all cases, excellent agreement was obtained using Eq. (7).

IV. Conclusions

Based on the work described in this paper, the following conclusions may be drawn:

1) The total pressure recovery of an exlet (a downstream exhaust nozzle used as an inlet) can be accurately described by using a semiempirical expression containing two loss coefficients: one coefficient for internal flow losses and one coefficient for external flow losses.

2) The internal loss coefficient can be experimentally determined in a static mode of exlet operation.

3) The external loss coefficient can be calculated from existing cone wake pressure data.

4) In low-speed operation, the exlet should be flared to about 30 deg for best performance.

Acknowledgments

It should be mentioned that this work was performed while two of the authors were employed by the NASA Lewis Research Center. Moreover, the authors are indebted to R. Luidens of NASA Lewis for his many helpful suggestions and encouragement over the course of this investigation.

References

[1] Dietrich, D.A., Keith, T.G., Jr., and Kelm, G.G., "Experimental Aerodynamic Performance of Flared Fan Nozzles Used as Inlets," NASA TMX-3367, March 1976.

[2] Vier, W.F., "Quiet, Clean, Short-Haul Experimental Engine (QSCEE) Test Results from a 14cm Inlet for a Variable Pitch Fan Thrust Reverser," General Electric Co., NAS3-18021, NASA, CR-134867, 1975.

[3] Fradenburg, E.A. and Wyatt, D.D., "Theoretical Performance Characteristics of Sharp-Lip Inlets," NACA TN-3004, 1953.

[4] Keith, T.G., Jr., "Subsonic Flow in a Downstream Facing Inlet," *Journal of Aircraft*, Vol. 11, April 1974, pp. 251-252.

[5] Obee, T.N., "Flow Patterns in the Vicinity of a Downstream Facing Inlet," M.S. Thesis, University of Toledo, Toledo, Ohio, 1976.

[6] Hoerner, S.F., *Fluid-Dynamic Drag*, Hoerner Publishing, Midland Park, N.J., 1965, pp. 3-18.

[7] Massey, B.S., *Mechanics of Fluids*, D. Van Nostrand Company, Princeton, N.J., 1968, p. 187.